

Mini Review

Refractive index as an intrinsic imaging contrast for 3-D label-free live cell imaging

Doyeon Kim¹, SangYun Lee², Moosung Lee², JunTaek Oh², Su-A Yang³, and YongKeun Park^{2,4,5,*}

¹*Department of Chemistry, Korea Advanced Institute of Science and Technology (KAIST), Daejeon 34141, South Korea*

²*Department of Physics, KAIST, Daejeon 34141, South Korea*

³*Department of Biological Sciences, KAIST, Daejeon 34141, South Korea*

⁴*KAIST Institute Health Science and Technology, Daejeon 34141, South Korea*

⁵*Tomocube Inc., Daejeon 34051, South Korea*

*Corresponding author, E-mail: yk.park@kaist.ac.kr, Phone: +82-42-350-2514, Fax: +82-42-350-2510

Abstract

Live cell imaging provides critical information in the investigation of cell biology and related pathophysiology. Refractive index (RI) can serve as intrinsic optical imaging contrast for 3-D label-free and quantitative live cell imaging, and provide invaluable information to understand various dynamics of cells and tissues for the study of numerous fields. Recently significant advances have been made in imaging methods and analysis approaches utilizing RI, which are now being transferred to biological and medical research fields, providing novel approaches to investigate the pathophysiology of cells. To provide insight how RI can be used as an imaging contrast for bioimaging, here we provide the basic principle of RI-based imaging techniques and summarize recent progress on applications, ranging from microbiology, hematology, infectious diseases, hematology, and histopathology.

Keywords: Bioimaging, Microscopy, Live cell imaging, Refractive index, Quantitative Phase Imaging, Holotomography

Impact Statement

The use of refractive index has been utilized for label-free and quantitative imaging contrast of cells and tissues. This mini review presents the principles of imaging techniques which exploit refractive index as an intrinsic optical imaging contrast, discusses the advantages and challenges, and summarize recent progress in various fields of biology and medicine.

Introduction

Optical images of biological cells and tissues provide invaluable information on the pathophysiology of diseases. Visual diagnosis of blood cells is essential for the diagnosis of various infectious diseases associated with red blood cells. In pathology and cytology, tissue biopsy and morphological examination of cells, such as checking for abnormally shaped nuclei in Papanicolaou test, is an essential step for cancer diagnosis.

The medical diagnostic capabilities of various diseases have evolved with advances in optical imaging technology. In the 17th century, Robert Hooke first observed cork cells using his microscope. Since then, various types of microscopes have been developed and likewise the ability to investigate disease-related cellular, and cellular structures have dramatically improved in recent decades. For example, the invention of phase contrast and differential interference contrast microscopes in the mid 20th century have accelerated the studies in the field of microbiology and cell biology, because these interferometric microscopy techniques allowed effective visualization of transparent biological cells(1, 2). The development of fluorescent proteins and fluorescence microscopy have also enabled specific labeling of target molecules or proteins. This breakthrough in technology thus has opened a new era for molecular biology. Moreover, various super-resolution microscope

techniques have broken the barrier of diffraction-limited optical resolution. The resolution limit of the optical microscope has been extended to the nanometer scale, enabling investigation of biological phenomena at the single molecule scale (3, 4). More recently, researchers have used adaptive optical approaches for *in vivo* imaging of biological cells or tissues (5-7).

There are two factors to consider for bio-imaging technology: (i) what parameters should be used as the imaging contrast, and (ii) how the optical imaging system is used to map the distribution of this imaging contrast onto the image plane. Over the past several decades, fluorescent protein technology has been widely used to locate specific target molecules and proteins in cells using the molecular specificity of the probe. This allows effective visualization of specific targets in cells and tissues with very high imaging contrast. When combined with the fluorescence correlation spectroscopy technique, the fluorescent probe can also provide information about the physical and chemical information of the surrounding medium(8). In addition, when combined with the Foster resonance energy transfer technique, the intermolecular distance can be accurately measured in nanometer scale (9).

However, the use of fluorescent probes in bioimaging inevitably causes several limitations. It is important to note that fluorescence technology uses exogenous fluorescent molecules as a secondary imaging contrast. Expression or binding of a target molecule of a fluorescent probe in a cell generates various problems. First, the introduction of an exogenous marker into a cell can affect the intrinsic physiology of the cell, because of possible photodamage and phototoxicity caused by the fluorescent molecule. This issue becomes even more severe when experimenting with neurons or stem cells because these cells are more sensitive to changes in the environment. Second, long-term cell imaging may be limited when using fluorescent technologies due to photobleaching of probes. Common fluorescent probes cannot produce strong, continuous fluorescence signals. Most probes photobleach after some time, which means the probes irreversibly lose its fluorescence. Thus maximum time period for long-term imaging of live cells is limited to the photobleaching period of fluorescent probes. Third, most fluorescence technologies do not provide quantitative information. The use of fluorescent probes only provides information of the location of the target molecule, but it does not provide quantified information of the mass or concentration of the target molecule.

To complement the limitation caused by the use of exogenous imaging contrast, the use of refractive index (RI), as an intrinsic optical parameter has been exploited recently. All materials have unique RI value, which is correlated with the electrical permittivity of the material. RI is the ratio of the speed of light passing through the specific material to that passing in the vacuum. Conventional phase contrast or differential interference microscopy uses RI values as optical imaging contrast. However, their imaging systems do not provide a one-to-one quantitative mapping of the information about RI distributions in a sample, but only generate high contrast intensity information via interference. Recently, there have been escalating interests in measuring 3D RI distributions for various applications in bioimaging. Mainly because RI, as the primarily intrinsic optical parameters, provides the possibility for label-free live cell imaging with the capability of providing quantitative information about the sample. In this mini-review, we introduce the principle of optical techniques that measure 3D RI tomograms and summarize recent applications for the study of various biological and medical applications.

The principles of bioimaging using refractive index as imaging contrast

The RI of material is obtained by measuring the interactions between light and matter. One of the well-known RI measuring techniques includes a refractometer that obtains the average RI value of a solution or a surface plasmonic sensor used to measure the surface RI of metal. These refractometer techniques are suitable for measuring a sample with the homogeneous distribution of RI values, such as a transparent solution. However, it is technically challenging to measure a sample with an inhomogeneous distribution of RI values, such as biological cells or tissues. This is because light refracts and reflects at the interface between the two media with different refractive indexes. When light refraction and reflection occurs many times, the coherence summation of these events can be expressed as multiple light scattering. This explains why biological tissues appear opaque white, while individual cells seem transparent.

Conventionally, phase contrast or differential interference microscopy have been utilized to exploit the refractive index distributions in samples. When a laser beam passes through a transparent specimen, such as individual biological cells, the laser beam acquires a distorted wavefront or a phase information. This occurs because the speed of light passing through a specific part of the sample differs from another part due to inhomogeneous distribution of RI of the sample. Unfortunately, conventional image sensors do not directly measure this wavefront information, because the speed of light is much faster than the capturing ability of an image sensor. Thus, phase contrast or differential interference microscopy exploits the principle of light interference. Significant light interference can be created in an optical imaging system, such as a bright-field microscopy, by inserting additional optical components. This allows conversion of wavefront information into an intensity information that can be measured by an image sensor. This is how one can achieve high imaging contrast when imaging transparent biological cells using phase contrast or differential interference microscopy. Hence phase contrast or differential interference microscopy enables clear visualization of the boundaries of the cell membrane as well as subcellular organelles.

However, these conventional interference microscopes, such as phase contrast or differential interference microscopy, can only provide qualitative information. This is because the relationship between wavefront information and intensity images for these interference microscopes is not straightforward, thus making it difficult to extract quantitative information. Quantitative phase information can provide valuable information about the sample without using exogenous labeling agents. For example, the measurements of quantitative phase maps of red blood cells can be directly converted into a cell height information.

Various quantitative phase imaging (QPI) techniques have been developed and utilized for various research fields. In particular, Mach-Zehnder or Michelson types of interference microscopic techniques have been extensively utilized. In-line holography techniques simplify the optical setup by removing a reference arm. Quantitative phase microscopy techniques based on the transport of intensity or ptychography have provided enhanced imaging quality with relatively simple instrumentations. Recently, the QPI unit was developed as a filter-type add-on unit, which can be attached to an existing microscopy to convert a conventional bright-field microscope into a quantitative phase microscope(10). The detailed information on QPI and its application to biological studies can be found in elsewhere(11-13).

Principle of measuring 3D RI tomography of cells and tissues

Even though 2-D QPI techniques provide quantitative and label-free imaging of live cells, they only provide topographic information; i.e. the measured optical phase delay is a coupled parameter of cell height and its refractive index distribution. Thus, 2-D QPI techniques do not directly provide information about internal structures of cells, or tomographic information.

In order to measure 3-D RI tomograms of cells, one important step should be added to QPI. Multiple 2-D holograms of a cell should be measured at various angles of illuminations. Then, from these measurements, a 3D RI tomogram of the cell can be reconstructed via inverse scattering theory. This technique is also known as optical diffraction tomography (ODT) and holotomography (HT). The principle of 3-D RI tomography is very similar to X-ray computed tomography (CT) where multiple 2-D X-ray images of the human body are measured at various illumination angles, and a 3-D X-ray absorptivity tomogram is then retrieved via the inverse scattering theory. Both X-ray CT and laser HT shares the same governing equation – Helmholtz equation, the wave equation for a monochromatic wavelength.

The history of HT goes back to the late 60s. After the rise of X-ray CT technology and the invention of lasers, some pioneering physicists realized that the X-ray CT principle could also be applied to a laser. The principles of X-ray CT are based on wave propagation and can be described by the wave equation, except they use different wavelengths of waves. The first theoretical work was presented in 1969 by Emil Wolf (14), and the first experimental demonstration was shown in 1979 by Fercher et al.(15). However, it seems that at the time many researchers did not realize this HT technique can be applied to bioimaging with significant benefits. The early applications of HT technique had been limited to measuring 3-D shapes of transparent microscopic plastics. In the 2000s, several research groups have revised and employed the HT technique for biological applications(16-18).

HT technology directly provides the measurements of the 3-D RI distribution of a cell. The reconstruction of 3-D RI tomogram of the specimen is achieved by inversely solving the Helmholtz equation from a set of multiple 2-D optical field images of the sample. This set of 2-D optical field images of the sample containing the 3-D information is generally obtained by varying the illumination angle of a laser impinging onto the specimen(17, 19, 20), or rotating the specimen while keeping the light source fixed(21-23). For further information, please refer Ref. for the principle of HT technology. Reference(18) describes the detailed procedure of HT with a MatLab source code. Reference(24) summarize various regularization algorithms used in HT.

From a technical point of view, significant technical advancements have been made recently. For example, the sub-100-nm spatial resolution was achieved using the deconvolution of complex optical field(25). Tomographic RI reconstruction with white light illumination was presented, which demonstrates significant reduction of speckle noise and dramatically improved image quality(26). Hyperspectral HT was also demonstrated; it measures 3-D RI tomograms of a sample at various wavelengths using a wavelength scanning illumination(27). The real-time reconstruction and visualization were also demonstrated, which was powered by a graphic processor unit (GPU)(28). It is worthy to note that in the mid 2010s, HT technology was commercialized and had started being used in biological laboratories and medical hospitals. As of 2017, two companies are providing the commercialized HT systems – Nanolive (www.nanolive.ch) and Tomocube (www.tomocube.com).

Opportunities and challenges of RI as imaging contrast

Exploiting RI as imaging contrasts have several advantages and limitations. In this section, we summarize representative features of HT technology.

1. Label-free: Because RI is an intrinsic optical parameter of material. No labeling agents or dyes are required for imaging biological cells and tissues. It means 3-D images of live cells can be obtained for a long time as long as physiological conditions are met. In addition, it can save time and cost for sample preparation. This label-free feature might become powerful for some applications where cells are to be reinjected to human bodies, for example, as in immune therapy or stem cell therapy.
2. Quantitative bioimaging: Using HT technology, RI value can be precisely measured. Unlike fluorescence techniques, where the intensity of fluorescence emission highly depends on protocol and the results are only qualitative, HT technology provides highly reproducible RI value in a quantitative manner. Importantly, the RI value can be directly translated into the protein concentration information. Furthermore, the dry mass of subcellular structures or cells can also be calculated from RI distributions(29, 30).

HT technology also has several limitations and challenges:

1. Limited molecular specificity: Although RI values can be precisely measured using HT technology, it is difficult to relate these measured RI to molecular information. This is mainly because proteins have similar RI values regardless of their types. Nonetheless, the spatial distribution RI values can provide limited morphological information about subcellular organelles. For example, nucleus membrane, nucleoli, lipid droplets, and vacuoles can be easily identified from RI distributions because they have distinct RI values different from neighboring environments(29, 31). Furthermore, the gradient of RI can also be utilized for further discriminating subcellular structures.

With these potentials and challenges, measuring RI tomography of various types of cells have become widely adapted for the study of various research topics. Below we highlight recent applications of measuring RI tomograms for various research disciplines.

Microbiology

Observing individual bacteria with conventional optical microscopes is challenging. This is due to a number of reasons. One is the size of most bacteria, which are in the order of micrometers or smaller. In addition, bacterial cytoplasm has refractive indexes similar to that of a medium, and the bacteria are transparent. Therefore it is

difficult to visualize bacteria under a conventional bright field microscope and a high-resolution microscope is required.

When imaging a bacterial cell using a phase contrast microscope, it is possible to obtain good imaging contrast. In this case, however, only limited morphological information is provided, such as the length, width, and shape of bacterial cells. Although phase contrast microscopy can measure live bacteria without using labels, it has limited capability for the study of microbiology because it provides only 2D qualitative images. Immunofluorescent labeling technology can provide molecular-specific information inside bacteria, but it can be time-consuming and costly to stain the cells. In addition, research is limited due to secondary problems such as photochromism and phototoxicity that occur during the bleaching process. This makes it difficult to observe the bacteria for long periods of time. Traditionally, confocal microscopes and transmission electron microscopes have been used to obtain the internal structure of individual bacteria at high resolution. However, it is difficult to observe live cells for a long time because these techniques require cell staining or interception.

RI tomographic imaging techniques can solve the problems of these existing imaging techniques. Because it is a non-invasive, label-free method, living bacteria can be observed for a long time without using additional exogenous labeling agents. In particular, by measuring the RI, protein concentration and mass information within the bacteria can be extracted, which has recently led to several studies related to the division of bacterial cells. However, because RI itself does not provide molecular specific information, in-depth investigation in the context of molecular biology is significantly limited. In the future, there will be potentials where both 3D RI tomographic imaging and fluorescence microscope technique are used simultaneously.

Several previous papers had been reported where 3D RI tomograms of individual bacteria are measured using HT technology. Using Mach-Zehnder interferometer and illumination scanning, 3-D RI tomograms of bacteria extracted from a sample of stool(16) and *E. coli* (25) have been reported. Recently, white-light diffraction tomography was used to image 3-D RI tomogram of *E. coli*(26). More recently, 3-D RI distribution of *Magnetospirillum gryphiswaldense*, a magnetotactic bacterium which produces magnetic particles (magnetosome), were measured (32).

RI information can be exploited to retrieve cellular dry mass and concentration information about individual bacteria. Dry mass refers to the non-aqueous contents inside cells and can be used as an indicator of cellular growth and division. Because RI of cytoplasm is linearly proportional to its concentration, RI tomography represents protein distribution of a cell. Furthermore, the integration of RI over cell volume can also provide information about the dry mass of the cell. Dry mass of a cell can be simply retrieved by measuring 2-D optical phase delay maps and averaging it over cell area because the optical phase delay map of a cell corresponds to the integration of RI differences between non-aqueous contents inside cells(12, 30). The cellular dry mass of fission yeast was monitored during the cell cycle with digital holographic microscopy, and the difference of mass production rate between wild-type and mutant fission yeast cells was observed(33). Using spatial light interference microscopy (SLIM), the dry mass of *Escherichia coli* cells was measured(34). In this work, the roles of cell density and morphology in mass regulation had been investigated.

Hematology

The physical parameters of red blood cells (RBCs) are strongly related to the pathophysiology of various diseases(35). Conventionally, optical microscopy with labeling methods has been used to examine RBC morphology in blood smears; poikilocytosis (e.g. spherocytes, target cells) and blood-borne infectious diseases including malaria are routinely examined. Information about hemoglobin (Hb) in RBCs are of particular importance in laboratory medicine; mean corpuscular Hb concentration (MCHC) and mean corpuscular Hb content (MCH) are extensively examined for medical diagnosis. It is also well known that the deformability of RBCs can be altered by several infectious diseases and genetic disorders (e.g. malaria and sickle cell disease)(36-40), with the implications of malfunctions in microcirculation. In clinical hematology, automated blood cell counters based on the complete blood count (CBC) have been utilized to measure the properties of RBCs. Current automated blood cell counter techniques measures the parameters of RBCs, including mean corpuscular volume (MCV), MCHC, MCH, and RBC distribution width (RDW), which serve as the principal and crucial information from which clinicians diagnose abnormalities in RBCs.

The use of 3D RI tomography in the field of hematology could lead to the simultaneous measurements of various optical parameters of individual RBCs. Figure 1 summarizes the analysis procedure for retrieving the parameters of individual RBCs using 3D RI tomography, including the volume, surface area, sphericity, Hb content, Hb concentration, and membrane fluctuation, which can be obtained at the single cell level. Figure 1 summarizes the analytical procedure for retrieving the parameters of individual RBCs using 3D RI tomography, including volume, surface area, sphericity, Hb concentration, Hb content, and membrane fluctuations.

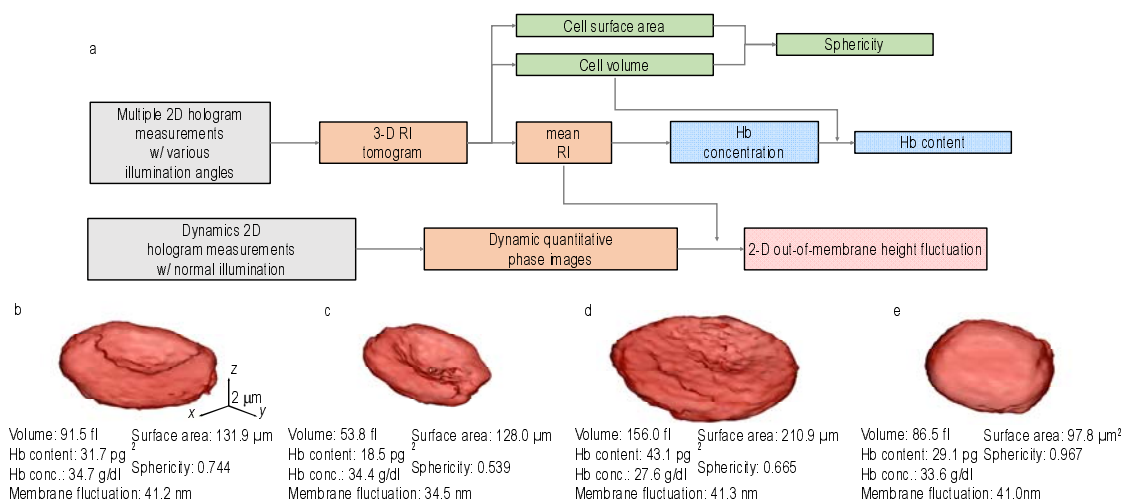


Figure 1. (a), Schematic diagram of the analysis procedure for retrieving the parameters of individual RBCs using 3D RI tomography. (b-d), 3D rendered isosurfaces of RI tomograms of individual RBCs and retrieved parameters from (b) healthy, (c) Iron-deficiency anemia, (d) reticulocyte, and (E) HS red blood cells. Reproduced from Ref. (39) with permission.

The measurements of various parameters of RBCs enables single-cell profiling, of which the importance has escalated in recent years(41). Regulation of dynamic cellular systems and related pathophysiology can be better understood when the various parameters of individual cells are simultaneously analyzed in detail. This is because of recent improvements in measurement techniques, which have made single-cell profiling more efficient than before. In addition, data-based research approaches in biology and medicine have also grown rapidly, allowing researchers to explore new perspectives, in addition to existing hypothesis-based research methods. 3D RI measurements enables the retrieval of morphological (cell volume, cell surface area, sphericity), biochemical (Hb content, Hb concentration), and biomechanical (dynamic membrane fluctuation) information measured at the individual cell level. This allows enables correlative analysis, which is not possible with the conventional automated blood cell counters.

Previously, 2-D QPI techniques have been employed for various applications in hematology. In particular, optical measurements of the parameters of individual RBCs have been widely studied, including malaria-infected human red blood cells(36, 42), sickle cell diseases(37, 43)⁴⁰, and ATP-dependent fluctuations(44). RBCs do not have subcellular organelles and exhibit homogeneous RI distributions, which therefore allows measurements of Hb concentration. Thus, 2-D QPI measurements can also provide both the morphological information (cell height map) as well as the biochemical information (Hb contents or dry mass), with a prior information about Hb concentration or the RI value of RBC cytoplasm. However, RBCs from an individual with diseases such as malaria infection or sickle cell anemia, the values of Hb concentrations, and thus RI values, vary significantly. Therefore, it is required to directly measure the 3D RI tomograms of individual RBCs for the systematic study of disease states.

Recently, 3D RI tomograms of RBCs have been utilized for measuring the parameters of individual RBCs. Lee et al. used common-path diffraction optical tomography (cDOT)(19), and measured 3-D RI tomograms and dynamic membrane fluctuations of RBCs exposed to ethanol(45), using common-path diffraction optical tomography(19). It was observed that RBCs exposed to an ethanol concentration of 0.1–0.3% v/v becomes more spherical shapes than those of normal cells(45). Using the cDOT, the properties of individual RBCs stored with and without a preservation solution, citrate phosphate dextrose adenine-1 (CPDA-1) were reported. In this work, various red blood parameters were analyzed and the results showed that, in the absence of CPDA-1, RBCs undergo a dramatic morphological transformation from discocytes to spherocytes within two weeks(46). The RBCs also experienced reduction in cell surface areas and became less flexible. However, RBCs stored with CPDA-1 retained their biconcave shapes and deformability for up to six weeks.

More recently, the RBCs from patients with diabetes mellitus have been systematically measured using 3-D RI tomography and dynamic membrane fluctuations(47). Morphologies of the RBCs from diabetic patients were not significantly different from the healthy ones. The deformability of the RBCs from diabetic patients was significantly lower than those of healthy RBCs, which is consistent with the previous literature using ektacytometry or filtration assay. Interestingly, this work reported the negative correlation between dynamic membrane fluctuation and glycated Hb concentration or HbA1c level, for the healthy RBCs; the higher the HbA1c level, the less deformable the cells are. In addition, the alterations in RBCs resulted from the binding of mellittin, the active molecule of apitoxin or bee venom, have been studied by measuring 3-D RI maps and dynamic membrane fluctuations(48). RBCs from the cord blood of newborn infants and from adult mothers or nonpregnant women were also systematically studied using 3-D RI tomography(49).

The study of white blood cells using 3-D RI tomography has not been fully exploited, but it will open new applications. More recently, Yoon et al. measured 3-D RI tomograms of mouse lymphocytes and macrophage(50). In this work, the morphological alternations in lymphocytes, caused by lipopolysaccharide which is known to immunologically stimulate lymphocytes, were analyzed.

Infectious diseases

The visualizations of the structures and dynamism of parasites and host cells are important for the study of parasitic infections. Although electron microscopy techniques provide excellent spatial resolutions, which can even visualize the internal structures of parasites. However, the high spatial resolution of electron microscopy comes at the cost of static imaging; it does not provide the time-lapse information of parasitic infections. Optical microscopy techniques have been extensively used for imaging parasites and host cells(51). The use of labeling agents with high molecular specificity have elucidated the molecular biology of various infectious diseases. However, conventional fluorescent labeling techniques only provide qualitative imaging capability, and some parasite is difficult to be labeled.

Recently, 3-D RI tomography techniques have been utilized for the field of infectious diseases. Park et al. have used tomographic phase microscopy and measured 3-D RI maps and dynamic membrane fluctuations of malaria infected RBCs as a function of various infection stages(36). *Plasmodium falciparum* parasites invaded into host human red blood cells were clearly visualized from the measurements of 3-D RI tomography. In addition, the significantly decreased dynamic membrane fluctuations in the infected RBCs were also reported, indicating the decreased cell deformability. The label-free capability of 3-D RI tomography has been utilized for the study of egress of malaria parasites(42), which provided a comprehensive body of information on the relationships between biomechanical and biochemical parameters and parasite egress from RBCs infected by malaria-inducing parasites. Kim et al. employed the optical diffraction tomography (ODT) algorithm to reconstruct 3-D RI tomography of malaria infected RBCs and it shows better image quality compared to the ones obtained with optical projection algorithm because ODT considers light diffraction inside samples(18). In addition, various morphological information about invading parasites and produced hemozoin structures are obtained and analyzed quantitatively.

More recently, *Babesia microti* invaded RBCs were investigated by measuring 3-D RI tomograms at the individual cell level(52). *B. microti* causes emergency human babesiosis, which shares similar pathophysiology and pathologic symptoms with malaria. In this work, RI information was effectively used for the study of

babesiosis, because the RI of *B. microti* parasites is distinct from RBC cytoplasm can thus be clearly visualized, otherwise very difficult to be identified with conventional optical imaging techniques because of the lack of effective labeling agents for *B. microti* parasites. Ekpenyong et al. reported the RI maps of Primary murine bone marrow derived macrophages which were infected by *Salmonella enterica* serovar Typhimurium(53).

3-D RI tomography was also employed for the study of viral infection. Simon et al. used a setup, in which fluorescence confocal microscopy and optical diffraction tomography were combined, and studied human respiratory epithelial carcinoma A549 cells infected with human influenza H3N2 virus(54). Interestingly, in the infected cells, the spherical structures with the size of 150–200 nm and with the distinctly high RI values were observed, which were expected to correspond to the buddings of viral particles.

Hepatology

Optical microscopic imaging of hepatocytes has played an important role in hepatology. The structures of cells and subcellular organelles and their dynamics are strongly correlated to the physiology of hepatocytes, and also significantly altered associated with liver-related diseases. Recently, Kim et al. have measured 3-D RI tomograms of human hepatocytes (human hepatocellular carcinoma cell line, Huh-7) were measured at the individual cell level. In this work, various subcellular structures of hepatocytes are clearly identified using RI values, including cell membrane, nucleus membrane, nucleoli, and lipid droplets (LDs)(55). In addition, time-lapse 3-D RI tomograms of hepatocytes were also measured, from which dynamics of individual LDs were quantified.

Among subcellular structures of hepatocytes, lipid droplets (LDs) are of particular interest because they are directly related to the lipid metabolism. LDs consist of a monolayer of phospholipids and associated proteins surrounding a core of neutral lipid and are ubiquitous intracellular organelles storing and supplying lipids in most cell types as well as hepatocytes(56). Recent studies suggest that LDs participate in various pathological roles, such as cancer and diabetes mellitus, and exhibit 3-D motions to regulate lipid storage and metabolism(57). However, the detailed process of LDs dynamics including biogenesis, growth and 3-D subcellular motions are incomplete(58).

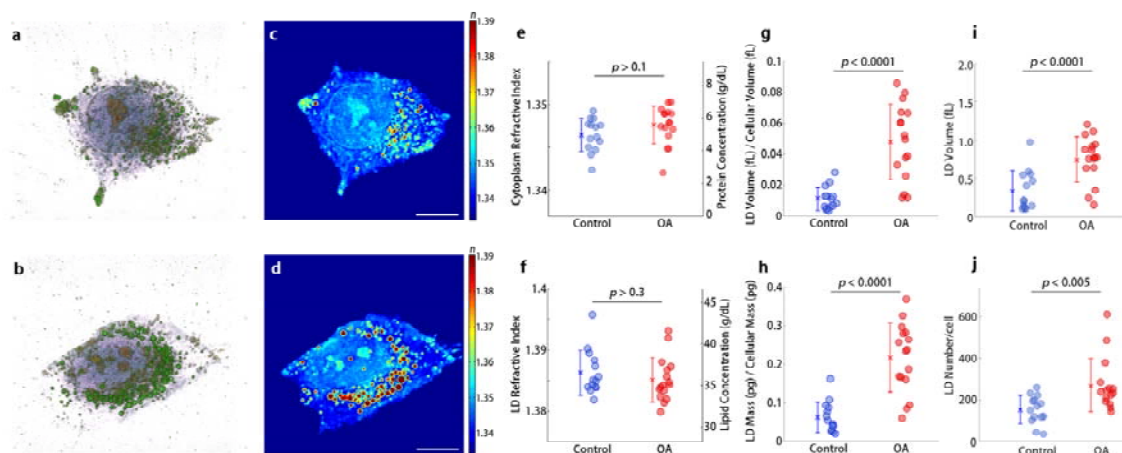


Figure 2. (a,b) 3-D rendered isosurface image of 3-D RI distribution of (a) an untreated and (b) oleic acid (OA) treated hepatocyte. (c,d) Cross-sectional slice images of 3-D RI distribution of (a) the untreated and (b) OA treated hepatocyte. The scale bars indicate $10 \mu\text{m}$. e-j, Quantitative analysis of (e) RI of cytoplasm, (f) RI of LDs, (g) the ratio of LD volume to cell volume, (h) the ratio of LD mass to cellular dry mass, (i) volume of individual LDs, and (j) number of LDs in untreated and OA-treated hepatocytes. Reproduced from Ref. X with permission

LDs can be effectively visualized exploiting its RI value; the RIs of lipid are significantly higher than protein(59) and thus LDs can be identified by measuring 3-D RI tomograms. Measuring LDs using the high RI values have several advantageous over conventional approaches. Fluorescence techniques for labeling LDs have been widely used(60), but the use of fluorescent probes requires for ethanol treatment, which can influence the physiological conditions of LDs such as induced fusions of LDs in live cells(61). Coherent anti-Stokes Raman scattering Raman scattering techniques have been used to visualize LDs in live cells without the use of exogenous labels(62, 63), but it requires for highly expensive laser and detection instruments and have the issue of low signal-to-noise ratio for molecules with low concentrations. The recent study demonstrated that the time-lapse 3-D RI distribution of LDs in live hepatocytes could be quantitatively analyzed with ODT(55). The shapes, sizes, and the masses of individual LDs in live hepatocytes were retrieved from the measured 3-D RI tomograms.

Histopathology

RI can potentially serve as important contrast in histopathology because (1) the use of RI for imaging tissue slides provide imaging contrast for the visualization of anatomical features in tissue slides otherwise invisible under conventional bright-field microscopy and (2) it does not require for the labeling process which can save time and cost. In addition, unlike conventional histopathology that relies on staining agents, the use of RI can provide quantitative criteria for pathologies in unlabeled biological tissues.

The RI information, for example, was used to quantify the weight loss in the inflammation-induced colitis(64). Besides the dry mass information, the measurements of optical phase delay maps of a tissue slice could precisely be utilized to extract the scattering parameters such as scattering coefficients (μ_s) and anisotropies (g)(65-67). This is because light scattering in tissue is caused by inhomogeneous distributions of RI, and thus as light passes through tissue, it undergoes significantly large events of light refraction and reflection, resulting in complex patterns of multiple light scattering. These scattering parameters have been employed to investigate the morphological alterations in prostate cancers (Figs. 3a-b)(68), breast cancers(69) and epithelial pre-cancers(70), which can be potentially utilized for diagnostic purposes.

Recently, the label-free tissue imaging capability by utilizing RI information was adapted to neuroscience. Optical phase delay maps of brain tissues were obtained for whole brain mouse tissue slides(71). The maps of scattering parameter (μ_s and g), extracted from the measured optical phase delay images of brain tissue, showed anatomical structures, comparable to the ones obtained with the conventional hematoxylin and eosin (H&E) staining method (**Figs. 3c-e**). Furthermore, these scattering parameter maps showed a statistical difference between the tissue slides from mice with Alzheimer's disease and the ones from healthy mice, indicating the structural alternations in the tissue.

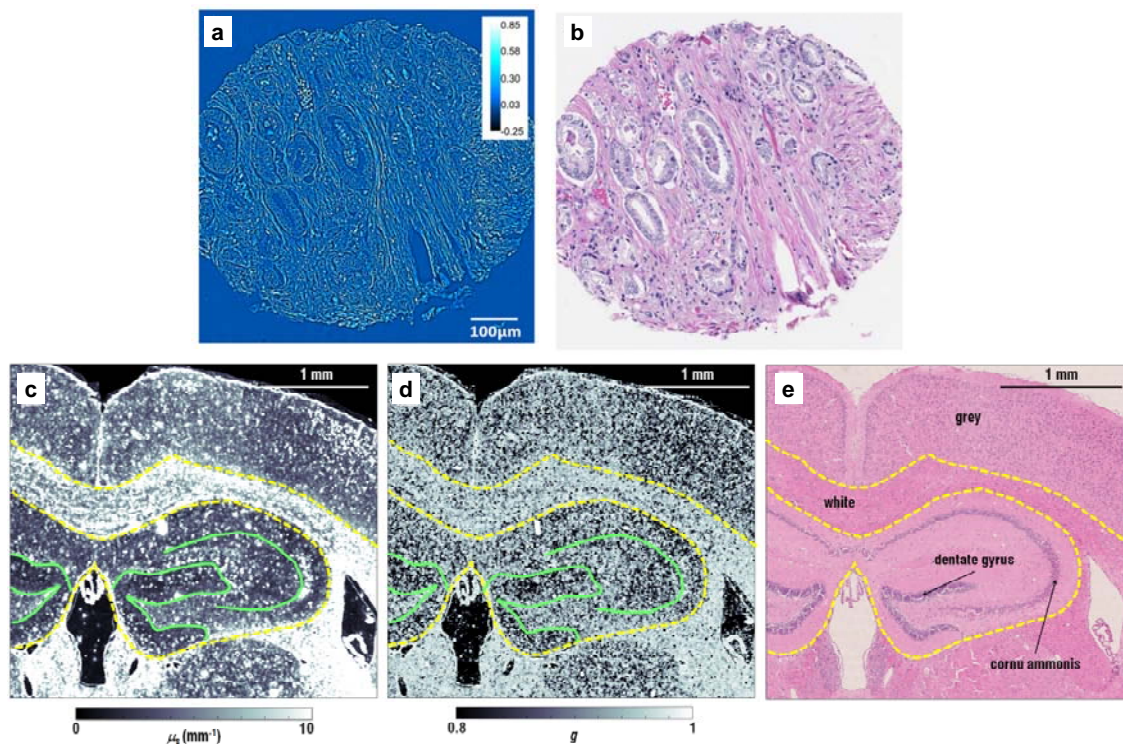


Figure 1. Applications of RI-based imaging techniques for histopathology and cell dynamics (a) Scattering parameter (μ_s) map and anisotropy (g) map of a whole mouse brain tissue slice, which was retrieved from the measured 2-D optical phase map of the slice. (c) The adjacent tissue slice labelled of (a-b) with conventional H&E staining. (d) 2-D optical phase map of a slice from a biopsy sample obtained from a patient who had biochemical recurrence of prostate cancer after undergoing radical prostatectomy. (e) The adjacent tissue slice of (d) labelled with conventional H&E staining. Reproduced from Refs. (71) and (68) with permission.

Outlook

Here we presented the principles of quantitative phase imaging techniques which exploit RI as an intrinsic optical imaging contrast for cells and tissues. Although this is a relatively new research field, and only a few topics of the studies have been investigated so far, the research work reviewed here suggest that the use of RI for bioimaging may play an important role in various fields of studies (summarized in Table 1), where label-free and quantitative live cell imaging capability provides benefits. This would significantly enhance our understanding of the pathophysiology of various diseases, which may also lead to the development of novel diagnostic strategies in the future.

Table 1. Major research areas which 2-D and 3-D RI measurement techniques have been employed.

Research Area	Application	Method	Reference
Microbiology	Magnetotactic bacterium (<i>Magnetospirillum gryphiswaldense</i>)	3-D RI imaging	(32)
	Cellular growth (fission yeast, <i>escherichia coli</i>)	Dry mass measurement from 2-D optical phase delay map	(33, 34)
	Bacterial identification (<i>escherichia coli</i> , <i>listeria monocytogenes</i> , <i>lactobacillus casei</i> , <i>bacillus subtilis</i> , <i>synechococcus elongatus</i>)	Fourier transform light scattering with 2-D optical phase delay map	(72, 73)

Hematology	Effect of external stimulus (ethanol, preservation solution)	2-D optical phase delay and 3-D RI imaging	(45, 46)
	Infectious disease (malaria, babesiosis)	2-D optical phase delay and 3-D RI imaging	(18, 74)
	Chronic human disease (sickle cell anemia, diabetes mellitus)	2-D optical phase delay and 3-D RI imaging	(75, 76)
	White blood cell	3-D RI imaging	(50)
Hepatology	Lipid droplets in Huh-7 (human hepatocellular carcinoma cell line)	3-D RI imaging	(55)
Histopathology	Colitis	2-D optical phase delay imaging	(64)
	Cancer (prostate, breast, and epithelial)	Scattering parameter measurement from 2-D optical phase delay map	(68-70)
	Neurological disorder (Alzheimer's disease and Parkinson's disease)	Scattering parameter measurement from 2-D optical phase delay map and 3-D RI imaging	(71, 77)
Cell dynamics	Intracellular diffusion (vesicles, organelles, and lipid droplets)	2-D optical phase delay and 3-D RI imaging	(55, 78)
	Membrane fluctuation (red blood cell)	2-D optical phase delay imaging	(44)
	Cell migration (red blood cell and cancer cell)	2-D optical phase delay and 3-D RI imaging	(79, 80)

The uses of RI as intrinsic imaging contrast for cells and tissues for biological and medical applications have not yet been fully explored; there are still various important issues in the physiology and pathology, which can be addressed by the utilization of RI-based imaging techniques and corresponding analysis methods. Some of the representative cell images in emerging fields are presented in Fig. 4. Many interesting studies which had been performed with 2-D QPI techniques would be readily investigated with 3-D RI tomography techniques because 3-D RI measurements directly provides both RI values and shape information, whereas 2-D QPI techniques only provide optical phase maps – a coupled parameter between RI values and the height of a sample. For example, water flux in individual neuron cells(81), morphologies of tumor cells(82), cell growth and division(34, 83, 84), and cell death(85) would be studied in more details with 3-D RI tomography.

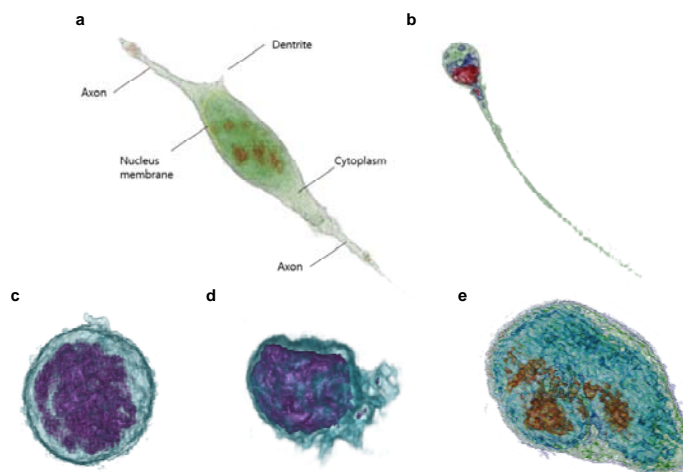


Figure 4. Emerging fields of research using 3-D RI tomography and representative cell images: (a) neuron cell; (b) human sperm; (c) mouse macrophage; (d) LPS-treated mouse macrophage; (e) embryonic stem cells. Image in (a) is reproduced from Ref. (77) with permission. Images in (b-e) are provided by Tomocube Inc

Stem cell research is one of the critical applications. Because 3-D RI tomography techniques enable label-free imaging of live cells while providing detailed morphological information at sub-cellular resolution, it can be exploited to monitor and identify the types and conditions of derived cells, which may have no issues when applied to target organs *in vivo*. For the same reasons, the approaches using RI values can also be implemented

to immunotherapy, because the measurements of 3-D RI maps of immune cells may be used for the label-free identification of subtypes of the cells or the evaluation of immune responses at the individual cell level.

Toward this direction of label-free cell identification, the use of RI-based imaging approaches has high potentials because RI serves as a highly reproducible and yet quantitative imaging contrast. Although the use of conventional fluorescence-based imaging contrast provides extremely high molecular specificity and signal-to-background ratio in imaging, fluorescence intensity is qualitative and generally difficult to be reproducible, largely subject to the various parameters, including the characteristics of fluorescent molecules and the transfection and expression efficiency of a protocol.

The use of RI as bioimaging contrast can have synergistic effects when combined with machine learning or deep learning algorithms. When cleverly combined with an algorithm, the large amount data obtained for each individual cells can be effectively handled. Recently, RI-based information has been started to be exploited in combination with machine learning algorithms. For example, from the 2-D optical phase imaging of individual bacteria, the genus of various bacteria was distinguished using a machine learning algorithm(86, 87).

Toxicology is one of the promising fields where the use of RI information can bring impact. Exploiting the label-free imaging capability of the RI-based approaches, the minute response of live cells can be precisely, and quantitative addressed. Recently, 3-D RI tomography techniques were used to image individual neuron cells, and to investigate morphological and biochemical alterations in individual neuron cells associated with early neurotoxic effects in Parkinson's disease(77). In this work, to establish the *in vitro* disease model, 1-methyl-4-phenylpyridinium ion (MPP+), which is known to cause symptoms of Parkinson's disease, was applied to individual neurons. Early neurotoxic effects of MPP+ was systematically investigated using 3-D RI tomography.

Finally yet importantly potential topics in application would include the 3-D label-free imaging for the study of Protist. Previously, 3-D RI tomography has shown potentials for the in-depth investigation of amoeba(88) and phytoplankton(89).

To facilitate the application of RI-based imaging methods for toxicology and pharmaceutical industry, it is required to achieve a platform to obtain high-throughput data. Toward this direction, several research activities are currently ongoing. Kim et al., presented a method to significantly enhance the speed of 3-D RI tomography employing sparse illumination patterns and a graphic processor unit (GPU)(28). Sung et al. demonstrated a method to obtain 3-D RI tomography of cells flowing in a microfluidic channel; without rotating a sample nor illuminating different patterns, optical information to construct a 3-D RI tomogram is acquired from the translations of a sample in the channel(90). Also, optical manipulation and 3-D tracking of biological cells in microfluidic channels may also open new applications with combined with 3-D RI tomography(91).

Developments in new analysis algorithm are also required. Previously, the quantitative imaging capability of RI-based imaging had been limited to static analysis, including cellular dry mass, morphological, and biochemical information. The RI information can also be exploited in analyzing dynamics of cells and subcellular compartments. Measurements of time-lapse 3D RI tomograms of cells would accompany with the developments in analysis algorithm(78).

New techniques to effectively handle the large size of data are particularly needed to make RI-based imaging approaches even more useful. In order to perform analysis at the individual cellular level and reveal the details of the underlying mechanisms of diseases, at least dozens of cells should be measured in each experimental group. Then a technical issue arises – the sizes of tomogram files are enormously significant. For example, HT-1 series from Tomocube Inc., a commercialized 3-D holographic microscopy system, generate a data file with a 67 Mega voxels for one 3-D RI tomogram; the imaging volume is $84.3 \times 84.3 \times 41.4 \mu\text{m}$ with the pixel resolution of $112 \times 112 \times 356 \text{ nm}$ for x-, y-, and z- direction, respectively. With the single-precision (or single) data type, a single tomogram of 67 Mega voxels will have the size of 268 Mbyte. When a 4-D or time-lapse 3-D tomograms the frame number of 512 is recorded, the data size will be approximately 134 Gbyte. More advanced methods to transfer, handle, and store such large sized data will also be required in the future.

From a technical point of view, the combination of an RI-based imaging technique with fluorescent imaging techniques will open a new avenue for live cell imaging. Because both RI and fluorescence labeling provides unique and complementary information about cells, the simultaneous measurement will provide useful and

synergistic information. One scenario of applications to utilize such a multimodal system would be that a 3-D fluorescence image of a cell is obtained in the beginning to register the location of specific molecules or organelles. Then time-lapse 3-D RI tomograms of the sample for a long time so that the dynamics of registered so that identified organelles can be tracked for an extended period of time by avoiding the issue of phototoxicity and photodamage to the cell. Previously, the combination of a 2-D quantitative phase imaging technique with fluorescence microscopy(92) and the combination of a 3-D RI tomography with confocal fluorescence microscopy has been presented(93), respectively.

Furthermore, to provide better molecular sensitivity to RI-based imaging, multispectral approaches have been introduced recently(94). The use of multiple coherent lasers(95, 96) or wavelength-scanning illumination(97, 98) enabled measuring the optical phase maps as a function of wavelength, and this information was utilized for molecular imaging because certain molecules have distinct optical dispersion properties, i.e. different RI values as a function of wavelengths. Recently, 3-D RI tomography has been achieved for a large number of wavelengths using a super continuum source and a wavelength-scanning unit(27). Besides the technical difficulty, the major challenge in exploiting optical dispersion for molecular specificity is that most molecules present in cells do not exhibit strong optical dispersion except specific molecules such as Hb(94). Alternatively, the use of an ultraviolet light source was presented to better visualize chromosomes inside a cell(93). More recently, the use of gold nanoparticles (GNPs) has been utilized in RI-based imaging, because the strong light absorption and scattering of GNPs at a resonant wavelength enable high imaging contrast(99, 100).

In addition, optical trapping techniques can be combined with RI-based imaging techniques to revolutionize the way in which biologists approach questions in the field of cell-to-cell interaction and mechanobiology. Toward to this direction, the combination with 3-D RI tomography and optical manipulation techniques are beneficial. The optical tweezer technique has been shown to optically trap spherical particles, which aided to manipulate individual cells. Recently, 3-D RI tomography technique was combined with holographic optical tweezers, which demonstrates the 3-D dynamic imaging of the interaction of an optically trapped particle to a macrophage(101). More recently, the 3-D RI maps of biological cells were measured in order to actively control optical wavefront for trapping beams, and the demonstration of stable control of complex shapes objects such as RBCs and dimers was demonstrated(102).

One of the future directions of RI-based imaging would be toward *in vivo* application. If the use of RI information can be collected *in vivo*, it would bring significant impacts to the early diagnosis of various diseases. However, because of multiple light scattering in biological tissues deteriorate the delivery of optical information(5), the direct application of a simple optical imaging system would not be able to acquire clear images. Recently, 3-D RI tomograms of individual RBCs flowing through micro capillaries(79). However, in this work, the part of a thin mesentery tissue should be placed in a 3-D holographic microscopy. Ford et al. demonstrated *in vivo* phase imaging by collecting *en face* phase gradient images of thick scattering samples(103). More recently, Laforest et al. demonstrated *in vivo* phase imaging of retinal cells using transcleral illumination, which gives a dark-field configuration with a high numerical aperture(104).

Various research results, in which RI was utilized as imaging contrast, are highlighted in this review article. Nonetheless, we believe that there are still uncountable potential applications, which are not yet discovered. In order to fully explore the potential and capability of RI-based approaches, interdisciplinary collaborations between biologists, medical specialists, and physicists are crucial. Considering the recent rapid growth of the field and the potentials of the approach, we are optimistic that optical imaging techniques based on RI will play important roles in various topics of studies where label-free and quantitative live cell imaging is important.

Acknowledgement

This work was supported by KAIST, BK21+ program, and the National Research Foundation of Korea (2015R1A3A2066550, 2014M3C1A3052567, 2014K1A3A1A09063027).

Competing Financial Interests

Prof. Park has financial interests in Tomocube Inc., a company that commercializes optical diffraction tomography and quantitative phase imaging instruments.

References

1. Zernike F. Phase contrast, a new method for the microscopic observation of transparent objects. *Physica*. 1942;9(7):686-98.
2. Allen R, David G, Nomarski G. The zeiss-Nomarski differential interference equipment for transmitted-light microscopy. *Zeitschrift fur wissenschaftliche Mikroskopie und mikroskopische Technik*. 1969;69(4):193-221.
3. Huang B, Bates M, Zhuang X. Super resolution fluorescence microscopy. *Annual review of biochemistry*. 2009;78:993.
4. Hell SW. Far-field optical nanoscopy. *science*. 2007;316(5828):1153-8.
5. Yu H, Park J, Lee K, Yoon J, Kim K, Lee S, et al. Recent advances in wavefront shaping techniques for biomedical applications. *Current Applied Physics*. 2015;15(5):632-41.
6. Yu H, Jang J, Lim J, Park JH, Jang W, Kim JY, et al. Depth-enhanced 2-D optical coherence tomography using complex wavefront shaping. *Optics Express*. 2014;22(7):7514-23.
7. Ji N, Milkie DE, Betzig E. Adaptive optics via pupil segmentation for high-resolution imaging in biological tissues. *nature methods*. 2010;7(2):141-7.
8. Thompson NL. Fluorescence correlation spectroscopy. *Topics in fluorescence spectroscopy*: Springer; 2002. p. 337-78.
9. Roy R, Hohng S, Ha T. A practical guide to single-molecule FRET. *Nature methods*. 2008;5(6):507-16.
10. Lee K, Park Y. Quantitative phase imaging unit. *Optics Letters*. 2014;39(12):3630-3.
11. Popescu G. *Quantitative Phase Imaging of Cells and Tissues*: McGraw-Hill Professional; 2011.
12. Lee K, Kim K, Jung J, Heo JH, Cho S, Lee S, et al. Quantitative phase imaging techniques for the study of cell pathophysiology: from principles to applications. *Sensors*. 2013;13(4):4170-91.
13. Majeed H, Sridharan S, Mir M, Ma L, Min E, Jung W, et al. Quantitative phase imaging for medical diagnosis. *J Biophotonics*. 2016.
14. Wolf E. Three-dimensional structure determination of semi-transparent objects from holographic data. *Optics Communications*. 1969;1(4):153-6.
15. Fercher AF, Bartelt H, Becker H, Wiltschko E. Image-Formation by Inversion of Scattered Field Data - Experiments and Computational Simulation. *Applied Optics*. 1979;18(14):2427-39.
16. Lauer V. New approach to optical diffraction tomography yielding a vector equation of diffraction tomography and a novel tomographic microscope. *Journal of Microscopy*. 2002;205(2):165-76.
17. Choi W, Fang-Yen C, Badizadegan K, Oh S, Lue N, Dasari RR, et al. Tomographic phase microscopy. *Nature methods*. 2007;4(9):717-9.
18. Kim K, Yoon H-O, Diez-Silva M, Dao M, Dasari R, Park Y-K. High-resolution three-dimensional imaging of red blood cells parasitized by *Plasmodium falciparum* and *in situ* hemozoin crystals using optical diffraction tomography. *J Biomed Opt*. 2014;19(1):011005-12.
19. Kim Y, Shim H, Kim K, Park H, Heo JH, Yoon J, et al. Common-path diffraction optical tomography for investigation of three-dimensional structures and dynamics of biological cells. *Optics express*. 2014;22(9):10398-407.
20. Shin S, Kim K, Yoon J, Park Y. Active illumination using a digital micromirror device for quantitative phase imaging. *Optics Letters*. 2015;40(22):5407-10.
21. Barty A, Nugent K, Roberts A, Paganin D. Quantitative phase tomography. *Optics Communications*. 2000;175(4):329-36.
22. Charrière F, Marian A, Montfort F, Kuehn J, Colomb T, Cuche E, et al. Cell refractive index tomography by digital holographic microscopy. *Optics letters*. 2006;31(2):178-80.
23. Kuś A, Dudek M, Kemper B, Kujawińska M, Vollmer A. Tomographic phase microscopy of living three-dimensional cell cultures. *Journal of biomedical optics*. 2014;19(4):046009.
24. Lim J, Lee K, Jin KH, Shin S, Lee S, Park Y, et al. Comparative study of iterative reconstruction algorithms for missing cone problems in optical diffraction tomography. *Optics Express*. 2015;23(13):16933-48.
25. Cotte Y, Toy F, Jourdain P, Pavillon N, Boss D, Magistretti P, et al. Marker-free phase nanoscopy. *Nature Photonics*. 2013;7(2):113-7.
26. Kim T, Zhou R, Mir M, Babacan SD, Carney PS, Goddard LL, et al. White-light diffraction tomography of unlabelled live cells. *Nat Photon*. 2014;8(3):256-63.
27. Jung J, Kim K, Yoon J, Park Y. Hyperspectral optical diffraction tomography. *Optics Express*. 2016;24(3):2006-12.

28. Kim K, Kim KS, Park H, Ye JC, Park Y. Real-time visualization of 3-D dynamic microscopic objects using optical diffraction tomography. *Optics Express*. 2013;21(26):32269-78.
29. Barer R. Determination of dry mass, thickness, solid and water concentration in living cells. *Nature*. 1953;172(4389):1097-8.
30. Popescu G, Park Y, Lue N, Best-Popescu C, Deflores L, Dasari RR, et al. Optical imaging of cell mass and growth dynamics. *Am J Physiol Cell Physiol*. 2008;295(2):C538-44.
31. Schürmann M, Scholze J, Müller P, Guck J, Chan CJ. Cell nuclei have lower refractive index and mass density than cytoplasm. *J Biophotonics*. 2016.
32. Bennet M, Gur D, Yoon J, Park Y, Faivre D. A Bacteria-Based Remotely Tunable Photonic Device. *Advanced Optical Materials*. 2016.
33. Rappaz B, Cano E, Colomb T, Kuhn J, Depeursinge C, Simanis V, et al. Noninvasive characterization of the fission yeast cell cycle by monitoring dry mass with digital holographic microscopy. *Journal of Biomedical Optics*. 2009;14(3).
34. Mir M, Wang Z, Shen Z, Bednarz M, Bashir R, Golding I, et al. Optical measurement of cycle-dependent cell growth. *Proceedings of the National Academy of Sciences*. 2011;108(32):13124-9.
35. Suresh S. Mechanical response of human red blood cells in health and disease: some structure-property-function relationships. *J Mater Res*. 2006;21(8):1872.
36. Park Y, Diez-Silva M, Popescu G, Lykotrafitis G, Choi W, Feld MS, et al. Refractive index maps and membrane dynamics of human red blood cells parasitized by *Plasmodium falciparum*. *Proc Natl Acad Sci USA*. 2008;105(37):13730-5.
37. Byun H, Hillman TR, Higgins JM, Diez-Silva M, Peng Z, Dao M, et al. Optical measurement of biomechanical properties of individual erythrocytes from a sickle cell patient. *Acta Biomaterialia*. 2012.
38. Mills JP, Diez-Silva M, Quinn DJ, Dao M, Lang MJ, Tan KSW, et al. Effect of plasmodial RESA protein on deformability of human red blood cells harboring *Plasmodium falciparum*. *Proc Natl Acad Sci U S A*. 2007;104(22):9213-7.
39. Kim Y, Shim H, Kim K, Park H, Jang S, Park Y. Profiling individual human red blood cells using common-path diffraction optical tomography. *Scientific reports*. 2014;4.
40. Diez-Silva M, Park Y, Huang S, Bow H, Mercereau-Puijalon O, Deplaine G, et al. Pf155/RESA protein influences the dynamic microcirculatory behavior of ring-stage *Plasmodium falciparum* infected red blood cells. *Scientific reports*. 2012;2:614.
41. Weatherall DJ. Systems biology and red cells. *N Engl J Med*. 2011;364(4):376-7.
42. Chandramohanadas R, Park Y, Lui L, Li A, Quinn D, Liew K, et al. Biophysics of malarial parasite exit from infected erythrocytes. *PLoS One*. 2011;6(6):e20869.
43. Shaked NT. Quantitative phase microscopy of biological samples using a portable interferometer. *Opt Lett*. 2012;37(11):2016-8.
44. Park Y, Best CA, Auth T, Gov NS, Safran SA, Popescu G, et al. Metabolic remodeling of the human red blood cell membrane. *Proceedings of the National Academy of Sciences*. 2010;107(4):1289.
45. Lee SY, Park HJ, Best-Popescu C, Jang S, Park YK. The Effects of Ethanol on the Morphological and Biochemical Properties of Individual Human Red Blood Cells. *PLoS one*. 2015;10(12):e0145327.
46. Park H, Lee S, Ji M, Kim K, Son Y, Jang S, et al. Measuring cell surface area and deformability of individual human red blood cells over blood storage using quantitative phase imaging. *Scientific Reports*. 2016;6.
47. Lee S, Park H, Kim K, Sohn Y, Jang S, Park Y. Refractive index tomograms and dynamic membrane fluctuations of red blood cells from patients with diabetes mellitus. *bioRxiv*. 2016.
48. Hur J, Kim K, Lee S, Park H, Park Y. Melittin-induced alterations in morphology and deformability of human red blood cells using quantitative phase imaging techniques. *bioRxiv*. 2016:091991.
49. Park H, Ahn T, Kim K, Lee S, Kook SY, Lee D, et al. Three-dimensional refractive index tomograms and deformability of individual human red blood cells from cord blood of newborn infants and maternal blood. *J Biomed Opt*. 2015;20(11):111208.
50. Yoon J, Kim K, Park H, Choi C, Jang S, Park Y. Label-free characterization of white blood cells by measuring 3D refractive index maps. *Biomed Opt Express*. 2015;6(10):3865-75.
51. Cho S, Kim S, Kim Y, Park YK. Optical imaging techniques for the study of malaria. *Trends in biotechnology*. 2011;30(2):71-9.
52. Park H, Hong S-H, Kim K, Cho S-H, Lee W-J, Kim Y, et al. Characterizations of individual mouse red blood cells parasitized by *Babesia microti* using 3-D holographic microscopy. *arXiv preprint arXiv:150500832*. 2015.
53. Ekpenyong AE, Man SM, Achouri S, Bryant CE, Guck J, Chalut KJ. Bacterial infection of macrophages induces decrease in refractive index. *J Biophotonics*. 2013;6(5):393-7.

54. Simon B, Debailleul M, Beghin A, Tourneur Y, Haeblerlé O. High-resolution tomographic diffractive microscopy of biological samples. *J Biophotonics*. 2010;3(7):462-7.
55. Kim K, Lee S, Yoon J, Heo J, Choi C, Park Y. Three-dimensional label-free imaging and quantification of lipid droplets in live hepatocytes. *Scientific reports*. 2016;6:36815.
56. Martin S, Parton RG. Lipid droplets: a unified view of a dynamic organelle. *Nature reviews Molecular cell biology*. 2006;7(5):373-8.
57. Welte MA. Fat on the move: intracellular motion of lipid droplets. *Biochem Soc T*. 2009;37:991-6.
58. Wilfling F, Haas JT, Walther TC, Farese Jr RV. Lipid droplet biogenesis. *Current opinion in cell biology*. 2014;29:39-45.
59. Beuthan J, Minet O, Helfmann J, Herrig M, Müller G. The spatial variation of the refractive index in biological cells. *Physics in medicine and biology*. 1996;41(3):369.
60. Martin S, Driessen K, Nixon SJ, Zerial M, Parton RG. Regulated Localization of Rab18 to Lipid Droplets EFFECTS OF LIPOLYTIC STIMULATION AND INHIBITION OF LIPID DROPLET CATABOLISM. *Journal of Biological Chemistry*. 2005;280(51):42325-35.
61. Fukumoto S, Fujimoto T. Deformation of lipid droplets in fixed samples. *Histochem Cell Biol*. 2002;118(5):423-8.
62. Nan X, Cheng J-X, Xie XS. Vibrational imaging of lipid droplets in live fibroblast cells with coherent anti-Stokes Raman scattering microscopy. *Journal of lipid research*. 2003;44(11):2202-8.
63. Evans CL, Potma EO, Puoris' haag M, Côté D, Lin CP, Xie XS. Chemical imaging of tissue in vivo with video-rate coherent anti-Stokes Raman scattering microscopy. *P Natl Acad Sci USA*. 2005;102(46):16807-12.
64. Lenz P, Bettenworth D, Krausewitz P, Brückner M, Ketelhut S, von Bally G, et al. Digital holographic microscopy quantifies the degree of inflammation in experimental colitis. *Integrative Biology*. 2013;5(3):624-30.
65. Ding H, Wang Z, Liang X, Boppart SA, Tangella K, Popescu G. Measuring the scattering parameters of tissues from quantitative phase imaging of thin slices. *Optics letters*. 2011;36(12):2281-3.
66. Wang Z, Ding H, Popescu G. Scattering-phase theorem. *Optics letters*. 2011;36(7):1215-7.
67. Wang Z, Tangella K, Balla A, Popescu G. Tissue refractive index as marker of disease. *Journal of biomedical optics*. 2011;16(11):116017-1160177.
68. Sridharan S, Macias V, Tangella K, Kajdacsy-Balla A, Popescu G. Prediction of prostate cancer recurrence using quantitative phase imaging. *Scientific reports*. 2014;5:9976-.
69. Majeed H, Kandel ME, Han K, Luo Z, Macias V, Tangella K, et al. Breast cancer diagnosis using spatial light interference microscopy. *Journal of biomedical optics*. 2015;20(11):111210-.
70. Su J-W, Lin Y-H, Chiang C-P, Lee J-M, Hsieh C-M, Hsieh M-S, et al. Precancerous esophageal epithelia are associated with significantly increased scattering coefficients. *Biomed Opt Express*. 2015;6(10):3795-805.
71. Lee M, Lee E, Jung J, Yu H, Kim K, Lee S, et al. Label-free optical quantification of structural alterations in Alzheimer's disease. *Scientific reports*. 2016;6.
72. Jo Y, Jung J, Kim M-h, Park H, Kang S-J, Park Y. Label-free identification of individual bacteria using Fourier transform light scattering. *Optics express*. 2015;23(12):15792-805.
73. Jo Y, Jung J, Lee JW, Shin D, Park H, Nam KT, et al. Angle-resolved light scattering of individual rod-shaped bacteria based on Fourier transform light scattering. *Scientific reports*. 2014;4.
74. Park H, Hong SH, Kim K, Cho SH, Lee WJ, Kim Y, et al. Characterizations of individual mouse red blood cells parasitized by *Babesia microti* using 3-D holographic microscopy. *Scientific Reports*. 2015;5.
75. Jung J, Matemba LE, Lee K, Kazyoba PE, Yoon J, Massaga JJ, et al. Optical characterization of red blood cells from individuals with sickle cell trait and disease in Tanzania using quantitative phase imaging. *arXiv preprint arXiv:160406796*. 2016.
76. Lee S, Park H, Jang S, Yongkeun P. Refractive index tomograms and dynamic membrane fluctuations of red blood cells from patients with diabetes mellitus. *Blood*. 2016;128(22):4813-.
77. Yang S-A, Yoon J, Kim K, Park Y. Measurements of morphological and biochemical alterations in individual neuron cells associated with early neurotoxic effects in Parkinson's disease using optical diffraction tomography. *bioRxiv*. 2016.
78. Ma L, Rajshekhar G, Wang R, Bhaduri B, Sridharan S, Mir M, et al. Phase correlation imaging of unlabeled cell dynamics. *Scientific Reports*. 2016;6.
79. Kim K, Choe K, Park I, Kim P, Park Y. Holographic intravital microscopy for 2-D and 3-D imaging intact circulating blood cells in microcapillaries of live mice. *Scientific Reports*. 2016;6.
80. Dubois F, Yourassowsky C, Monnom O, Legros J-C, Debeir O, Van Ham P, et al. Digital holographic microscopy for the three-dimensional dynamic analysis of in vitro cancer cell migration. *Journal of biomedical optics*. 2006;11(5):054032--5.

81. Jourdain P, Pavillon N, Moratal C, Boss D, Rappaz B, Depeursinge C, et al. Determination of transmembrane water fluxes in neurons elicited by glutamate ionotropic receptors and by the cotransporters KCC2 and NKCC1: a digital holographic microscopy study. *The Journal of Neuroscience*. 2011;31(33):11846-54.
82. Kemper B, Carl D, Schnekenburger J, Bredebusch I, Schäfer M, Domschke W, et al. Investigation of living pancreas tumor cells by digital holographic microscopy. *Journal of Biomedical Optics*. 2006;11(3):034005--8.
83. Kemper B, Bauwens A, Vollmer A, Ketelhut S, Langehanenberg P, Müthing J, et al. Label-free quantitative cell division monitoring of endothelial cells by digital holographic microscopy. *Journal of Biomedical Optics*. 2010;15(3):036009--6.
84. Cooper KL, Oh S, Sung Y, Dasari RR, Kirschner MW, Tabin CJ. Multiple phases of chondrocyte enlargement underlie differences in skeletal proportions. *Nature*. 2013;495(7441):375-8.
85. Pavillon N, Kühn J, Moratal C, Jourdain P, Depeursinge C, Magistretti PJ, et al. Early cell death detection with digital holographic microscopy. *PloS one*. 2012;7(1):e30912.
86. Jo Y, Jung J, Kim MH, Park H, Kang SJ, Park Y. Label-free identification of individual bacteria using Fourier transform light scattering. *Optics Express*. 2015;23(12):15792-805.
87. Jo Y, Jung J, Lee JW, Shin D, Park H, Nam KT, et al. Angle-resolved light scattering of individual rod-shaped bacteria based on Fourier transform light scattering. *Scientific reports*. 2014;4:5090.
88. Charrière F, Pavillon N, Colomb T, Depeursinge C, Heger TJ, Mitchell EA, et al. Living specimen tomography by digital holographic microscopy: morphometry of testate amoeba. *Optics Express*. 2006;14(16):7005-13.
89. Lee S, Kim K, Mubarak A, Panduwirawan A, Lee K, Lee S, et al. High-Resolution 3-D Refractive Index Tomography and 2-D Synthetic Aperture Imaging of Live Phytoplankton. *Journal of the Optical Society of Korea*. 2014;18(6):691-7.
90. Sung Y, Lue N, Hamza B, Martel J, Irimia D, Dasari RR, et al. Three-dimensional holographic refractive-index measurement of continuously flowing cells in a microfluidic channel. *Phys Rev Appl*. 2014;1(1):014002.
91. Merola F, Miccio L, Memmolo P, Paturzo M, Grilli S, Ferraro P. Simultaneous optical manipulation, 3-D tracking, and imaging of micro-objects by digital holography in microfluidics. *IEEE Photonics Journal*. 2012;4(2):451-4.
92. Park Y, Popescu G, Badizadegan K, Dasari RR, Feld MS. Diffraction phase and fluorescence microscopy. *Opt Express*. 2006;14(18):8263-8.
93. Sung Y, Choi W, Lue N, Dasari RR, Yaqoob Z. Stain-free quantification of chromosomes in live cells using regularized tomographic phase microscopy. *PloS one*. 2012;7(11):e49502.
94. Jung J, Kim K, Yu H, Lee K, Lee S, Nahm S, et al. Biomedical applications of holographic microspectroscopy [Invited]. *Applied Optics*. 2014;53(27):G111-G22.
95. Park Y, Yamauchi T, Choi W, Dasari R, Feld MS. Spectroscopic phase microscopy for quantifying hemoglobin concentrations in intact red blood cells. *Optics Letters*. 2009;34(23):3668-70.
96. Jang Y, Jang J, Park Y. Dynamic spectroscopic phase microscopy for quantifying hemoglobin concentration and dynamic membrane fluctuation in red blood cells. *Optics Express*. 2012;20(9):9673-81.
97. Rinehart M, Zhu Y, Wax A. Quantitative phase spectroscopy. *Biomed Opt Express*. 2012;3(5):958-65.
98. Jung J, Jang J, Park Y. Spectro-refractometry of individual microscopic objects using swept-source quantitative phase imaging. *Anal Chem*. 2013.
99. Turko NA, Peled A, Shaked NT. Wide-field interferometric phase microscopy with molecular specificity using plasmonic nanoparticles. *Journal of biomedical optics*. 2013;18(11):111414-.
100. Kim D, Oh N, Kim K, Lee S, Park J, Park Y. Label-free high-resolution 3-D imaging of gold nanoparticles inside live cells using optical diffraction tomography. *bioRxiv*. 2016:097113.
101. Kim K, Yoon J, Park Y. Simultaneous 3D visualization and position tracking of optically trapped particles using optical diffraction tomography. *Optica*. 2015;2(4):343-6.
102. Kim K, Park Y. Tomographic active optical trapping of arbitrarily shaped objects by exploiting 3-D refractive index maps. *arXiv preprint arXiv:161100638*. 2016.
103. Ford TN, Chu KK, Mertz J. Phase-gradient microscopy in thick tissue with oblique back-illumination. *Nature Methods*. 2012;9(12):1195-7.
104. Laforest T, Carpentras D, Kowalczyk L, Behar-Cohen F, Moser C. Quantitative phase imaging of retinal cells. *arXiv preprint arXiv:170108854*. 2017.